Lossless Data Compression for Infrared Hyperspectral Sounders - An Overview

Bormin Huang[*], Hung-Lung Huang, Alok Ahuja, and Hao Chen

Cooperative Institute for Meteorological Satellite Studies

Space Science and Engineering Center

University of Wisconsin–Madison

Madison, WI 53706, USA

Timothy J. Schmit[1] and Roger W. Heymann[2]

NOAA, National Environmental Satellite, Data, and Information Service

[1]Office of Research and Applications

Madison, WI 53706, USA

[2]Office of Systems Development

Suitland, MD 20746, USA

Submitted to 20th International Conference on Interactive Information and Processing Systems (IIPS) for Meteorology, Oceanography, and Hydrology, 11–15 January 2004, Seattle, Washington.

October 2003

[*] Corresponding author E-mail: bormin@ssec.wisc.edu

Lossless Data Compression for Infrared Hyperspectral Sounders - An Overview

Bormin Huang*, Hung-Lung Huang, Alok Ahuja, and Hao Chen
CIMSS, University of Wisconsin-Madison

Timothy J. Schmit and Roger W. Heymann
NOAA, National Environmental Satellite, Data, and Information Service

Hyperspectral sounding data requires accuracy for useful retrieval of atmospheric temperature, moisture, trace gases, clouds, aerosols and surface properties. Therefore, compression of hyperspectral sounding data is better to be lossless or near lossless. Given the large volume of three-dimensional hyperspectral data that will be generated by the hyperspectral sounders such as AIRS, CrIS, IASI, GIFTS and HES instruments, the use of robust data compression techniques will be beneficial to data transfer and archive. This paper reviews wavelet-based lossless data compression schemes for the 3D hyperspectral data using 3D integer wavelet transforms followed by 3D EZW and 3D SPIHT zerotree coding schemes. We extend both zerotree coding schemes to take on any size of satellite data, each of whose dimensions need not be divisible by 2^N, where N is the layers of the wavelet decomposition being performed. The 2D wavelet-based JPEG-2000 compression scheme and some other prediction-based 2D lossless compression schemes such as CALIC and JPEG-LS are also investigated. Their compression ratios are presented.

1. INTRODUCTION

In the era of contemporary and future hyperspectral sounders such as Atmospheric Infrared Sounder (AIRS) (Aumann *et al.*, 2001), Cross-track Infrared Sounder (CrIS) (Bloom, 2001), Interferometer Atmospheric Sounding Instrument (IASI) (Phulpin *et al.*, 2002), Geosynchronous Imaging Fourier Transform Spectrometer (GIFTS) (Smith *et al.*, 2002), and Hyperspectral Environmental Suite (HES) (Huang *et al.*, 2003), better inference of the atmospheric, cloud and surface parameters is possible. A huge amount of three-dimensional (3D) hyperspectral data, consisting of one spectral and two spatial dimensions, is produced by the hyperspectral infrared sounders. For example, the HES is the next-generation NOAA/NESDIS Geostationary Operational Environmental Satellite (GOES) hyperspectral sounder slated to be launched in 2013 to replace the current 18-band GOES sounder. It would be either an interferometer or a grating sounder with hyperspectral resolution (over one thousand infrared channels with spectral widths on the order of 0.5 wavenumber), high temporal resolution (better than 1 hour), high spatial resolution (less than 10km) and hemispheric coverage. Given the large volume of 3D data that will be generated by a hyperspectral sounder each day, the use of robust data compression techniques will be beneficial to data transfer and archive.

While lossy compression leading to significant data loss of the hyperspectral *imaging* data, e.g. AVIRIS data (Abousleman, 1999), is usually acceptable by the human visual system, hyperspectral *sounding* data requires a much higher accuracy for useful retrieval of atmospheric temperature, moisture, trace gases, cloud, aerosol and surface properties. For instance, the observed signal to instrument noise ratio in infrared longwave channels may be over 400 in the clear sky cases, implying that the ratio of the

original data values to the lossy reconstructed error in those channels be much higher for retrieval of geophysical parameters without significant degradation. The allowable reconstructed error is visually imperceptible by the human eye. Therefore there is a need for lossless or near lossless compression of hyperspectral sounding data. In support of the NOAA HES data processing studies, we investigate into lossless compression of the hyperspectral sounding data. Although lossless compression of hyperspectral imaging data has long been studied in literature, the compression of hyperspectral sounding data has not been explored yet.

In this paper, we present a review of 3D lossless hyperspectral sounding data compression using various state-of-the-art lossless data compression schemes that are either integer wavelet transform based or predictor based. Wavelet zerotree coding schemes such as 2D EZW (Shapiro, 1993) and 2D SPIHT (Said *et al*., 1996), and 2D JPEG2000 (ISO/IEC, 2000) belong to the general class of wavelet based data compression schemes, whereas 2D JPEG-LS (ISO/IEC, 1999) and 2D CALIC (Wu, 1997) belong to the class of predictor based compression schemes. We extend both 2D EZW and 2D SPIHT to 3D for any size of 3D satellite data, each of whose dimensions need not be divisible by 2^N, where N is the layers of the wavelet decomposition being performed. For other 2D schemes such as JPEG2000, JPEG-LS, and CALIC, we transform the 3D data into 2D via a continuous scan.

The rest of the paper is arranged as follows. Section 2 describes the hyperspectral sounding data used in this study. Section 3 highlights the different compression schemes while Section 4 details their compression results on the hyperspectral sounding data. Section 5 summarizes the paper.

2. DATA

The hyperspectral sounding data could be generated from either an interferometer (e.g. CrIS, IASI, GIFTS) or a grating sounder (e.g. AIRS). To simulate the 3D GIFTS data, we have adopted and modified the NASA AIRS radiance observations on Sept. 6, 2002. The AIRS instrument aboard NASA's Aqua spacecraft employs a 49.5 degree cross-track scanning with a 1.1 degree instantaneous field of view to provide twice daily coverage of essentially the entire globe in a 1:30 PM sun synchronous orbit. The AIRS data includes 2378 infrared channels in the 3.74 to 15.4 μm region of the spectrum. A day's worth of AIRS data is divided into 240 granules, each of 6 minute durations. Each granule consists of 135 scan lines containing 90 cross-track footprints per san line; thus there are a total of 135 x 90 = 12,150 footprints per granule. The 16-bit raw radiances are converted into the brightness temperatures, and then scaled as unsigned 16-bit integers. To make the tested hyperspectral sounding data generic, 270 bad channels identified in the supplied AIRS channel properties file are excluded, assuming that they occur only in the AIRS sounder but not in other hyperspectral sounders. Each resulting granule is saved as a binary file, arranged as 2108 channels, 135 scan lines, and 90 pixels for each scan line. Ten granules, five daytime and five nighttime, are chosen from different geographical regions of the Earth. Their locations, UTC times, and local time adjustments are listed in Table 1. The data is available via anonymous ftp (ftp://ftp.ssec.wisc.edu /pub/bormin/HES). More information regarding the AIRS instrument maybe acquired from the NASA AIRS website (http://www-airs.jpl.nasa.gov).

Granule 9	00:53:31 UTC	-12 H	(Pacific Ocean, Daytime)
Granule 16	01:35:31 UTC	+2 H	(Europe, Nighttime)
Granule 60	05:59:31 UTC	+7 H	(Asia, Daytime)
Granule 82	08:11:31 UTC	-5 H	(North America, Nighttime)
Granule 120	11:59:31 UTC	-10 H	(Antarctica, Nighttime)
Granule 126	12:35:31 UTC	-0 H	(Africa, Daytime)
Granule 129	12:53:31 UTC	-2 H	(Arctic, Daytime)
Granule 151	15:05:31 UTC	+11 H	(Australia, Nighttime)
Granule 182	18:11:31 UTC	+8 H	(Asia, Nighttime)
Granule 193	19:17:31 UTC	-7 H	(North America, Daytime)

Table 1. Ten selected AIRS granules for hyperspectral sounding data compression studies.

Figure 1 shows the AIRS radiances at wavenumber 900.3 cm^{-1} for the 10 selected granules on Sept. 6, 2002. In these granules, coast lines are depicted as solid curves and multiple clouds at various altitudes are shown as different shades of white pixels.

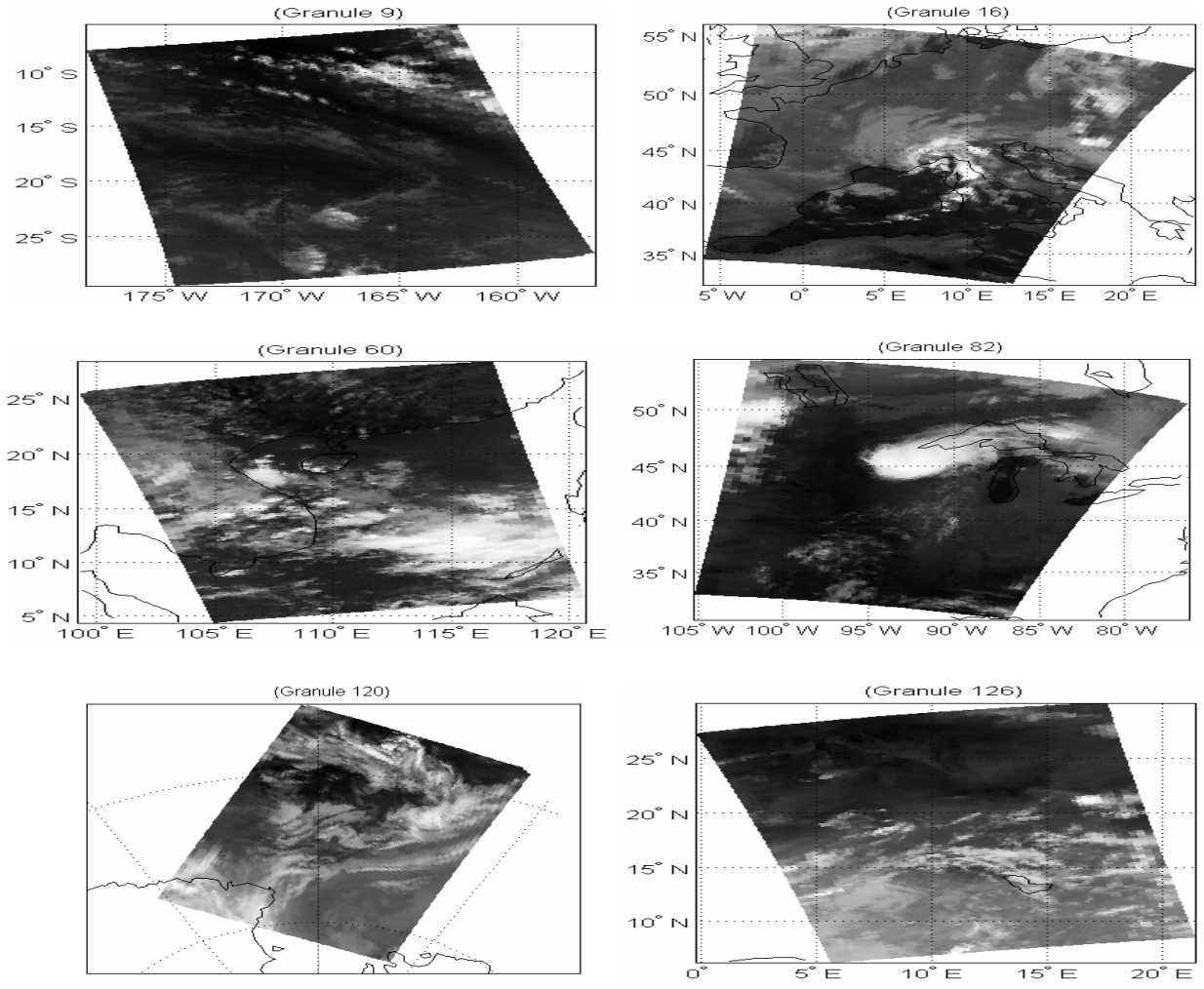

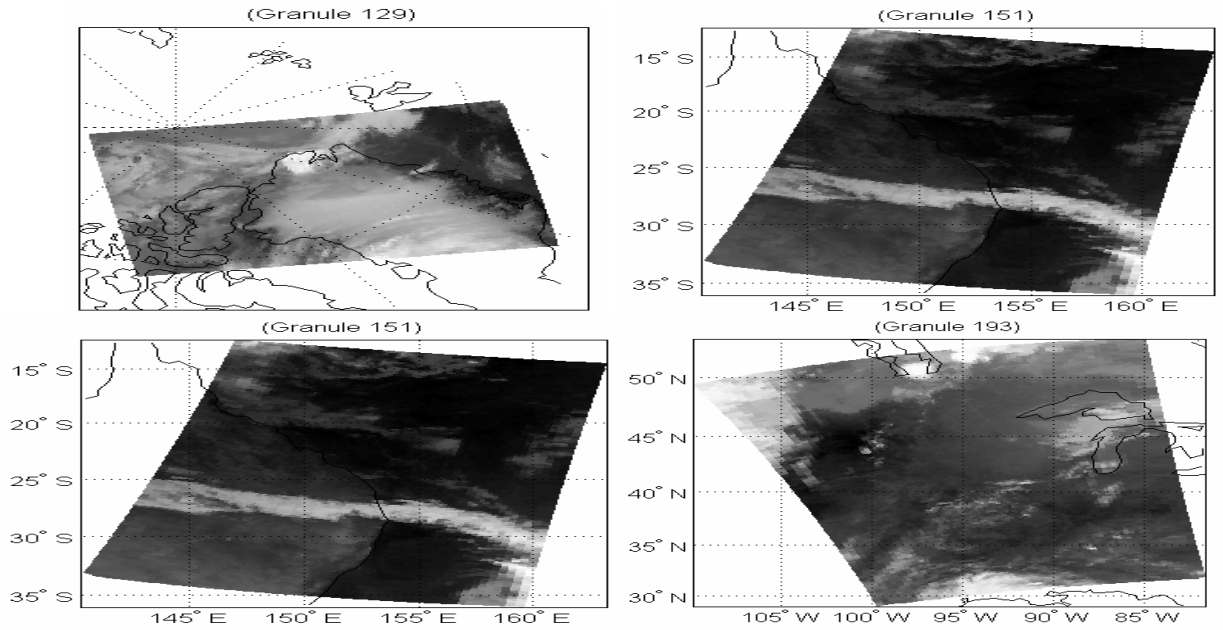

Fig. 1. AIRS radiance at wavenumber 900.3cm^{-1} for the 10 selected granules on Sept. 6, 2002.

Figure 2(a) shows all the 12150 radiance spectra (135 scan lines x 90 pixels) in granule 82. For comparison Fig.2(b) shows the calibrated noise spectrum converted from the noise equivalent temperature provided in the AIRS channel properties file. As can be seen, each infrared spectrum spans several orders of magnitude in radiance ranging from longwave to shortwave regions and each channel has various degree of signal-to-noise ratio.

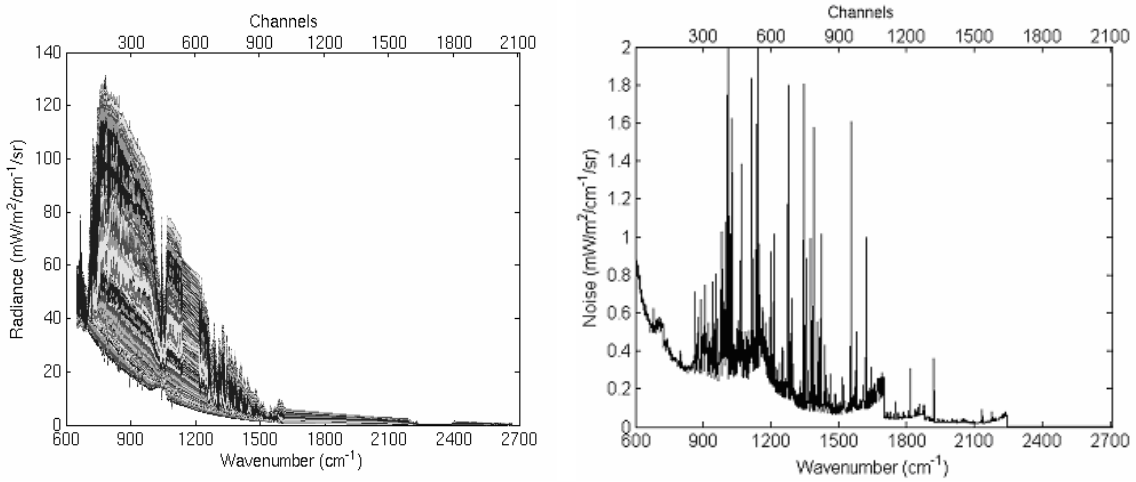

(a) (b)

Fig. 2. (a) 12150 observed AIRS radiance spectra in granule 82 on September 6, 2002. For generic hyperspectral sounder data compression studies, 270 bad channels out of the original 2378 AIRS channels have been removed. (b) AIRS calibrated noise spectrum for granule 82.

3. COMPRESSION SCHEMES

We investigate into both the wavelet transform based and predictor based schemes for lossless compression of the 3D hyperspectral sounding data. These are highlighted below.

3.1 Wavelet Based Schemes: The wavelet transform has been a successful tool in image compression. It features multi-resolution analysis with compact support and linear computation times. As a technique for image compression, the transform consists of a set of basis functions onto which the image is projected, and the resultant coefficients are then encoded. Wavelet compression exploits redundancies in scale to reduce the information stored in the wavelet domain. Integer wavelet transforms that map integers to integers are reversible in finite-precision arithmetic and hence have important applications in lossless data compression.

3.1.1 Integer Wavelet Transforms: The integer wavelet transform (DWT) can be implemented with the use of the lifting scheme (Daubechies *et al*., 1998). The lifting scheme has several desirable advantages that include low complexity, linear execution time and in-place computation, and it can be used on signals with an arbitrary length. The integer wavelet transform consists of three steps:

1) the lazy wavelet transform:

$$h_0[n] = x[2n+1],$$

$$l_0[n] = x[2n].$$

2) one or more dual and primal lifting steps:

$$h_i[n] = h_{i-1}[n] - \left\lfloor \left(\sum_k s_i[k]\, l_{i-1}[n-k] \right) + \frac{1}{2} \right\rfloor,$$

$$l_i[n] = l_{i-1}[n] - \left\lfloor \left(\sum_k t_i[k]\, h_i[n-k] \right) + \frac{1}{2} \right\rfloor.$$

where the filter coefficients $s_i[k]$ and $t_i[k]$ are computed by factorization of a polyphase matrix of any perfect reconstruction filter bank.

3) rescaling:

$$l[n] = \frac{l_N[n]}{K},$$

$$h[n] = K \cdot h_N[n].$$

The inverse is obtained by reversing the lifting and dual-lifting steps with the corresponding sign flips as:

$$l_{i-1}[n] = l_i[n] + \left\lfloor \left(\sum_k t_i[k]\, h_i[n-k] \right) + \frac{1}{2} \right\rfloor,$$

$$h_{i-1}[n] = h_i[n] + \left\lfloor \left(\sum_k s_i[k]\, l_{i-1}[n-k] \right) + \frac{1}{2} \right\rfloor .$$

The filter coefficients need not be integers, but are generally rational with power-of-two denominators allowing all divisions to be implemented using binary shifts. Figures 3 and 4 show the forward and inverse wavelet transforms using the lifting scheme, respectively.

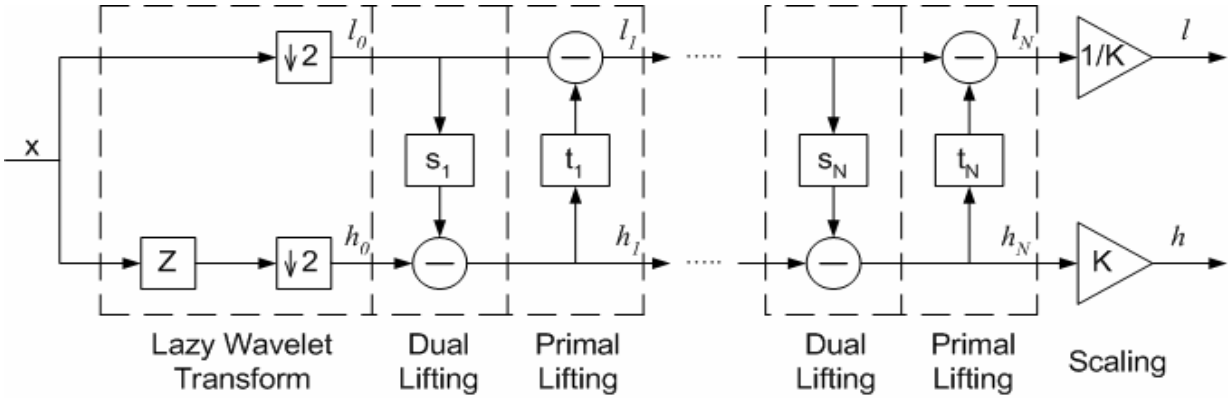

Figure 3. Forward wavelet transform using the lifting scheme.

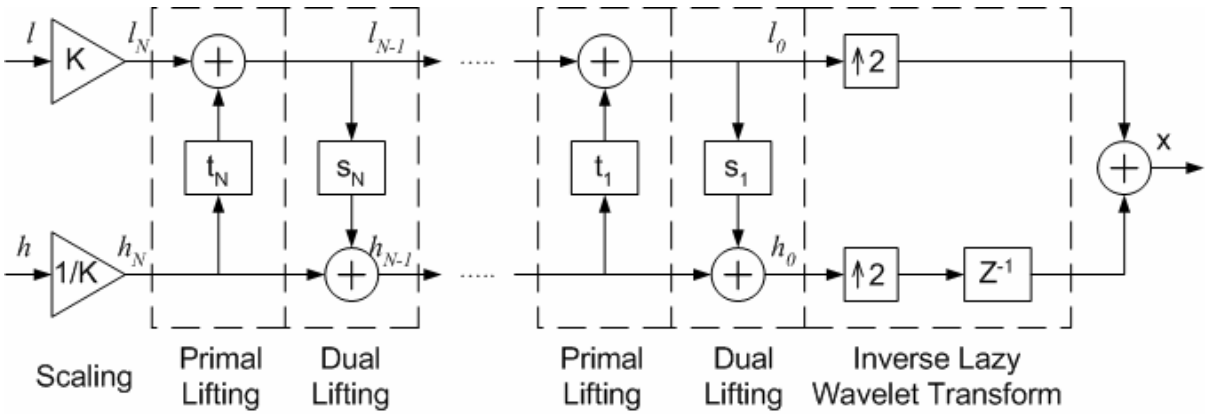

Figure 4. Inverse wavelet transform using the lifting scheme.

3.1.2 EZW and SPIHT: After the wavelet transform, the coefficients can be represented by use of a tree structure. Both the embedded zerotree wavelet (EZW) scheme and the Set Partitioning in Hierarchical Trees (SPIHT) take advantage of this structure for better compression. Different levels in the hierarchical subbands but at the same spatial orientation, display similar characteristics.

EZW uses this characteristic of multi-level wavelet transforms to efficiently encode the wavelet coefficients by defining the parent-child interband relationships in the decomposition structure.

SPIHT is a refinement of the EZW scheme which provides a better compression while also having faster encoding and decoding times. It uses spatially oriented trees to describe the relationship between the parents on higher levels to the children and grandchildren on lower levels. These spatial relationship trees are common for both

SPIHT and EZW and can be seen in the 3D wavelet decomposition of Fig. 5.

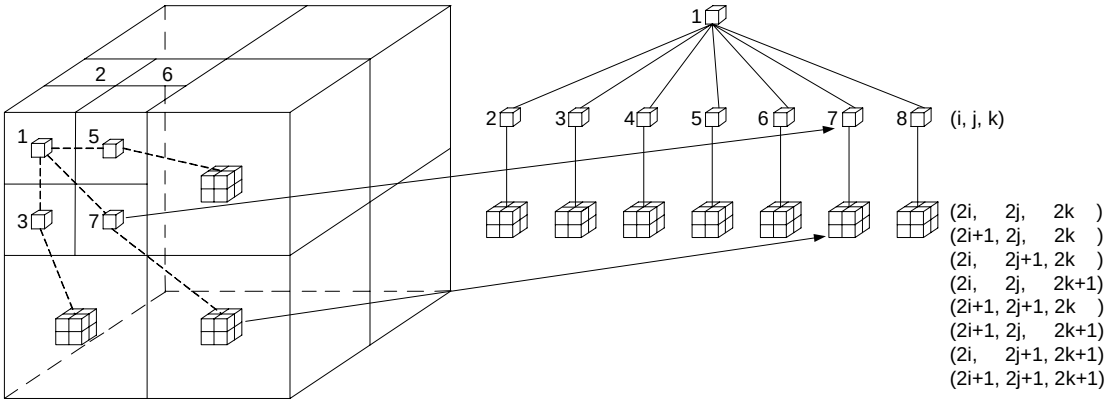

Figure 5. Parent-child interband relationship and locations for EZW and SPIHT coding

3.1.3 JPEG2000: This algorithm is published as a new standard of ISO/IEC, as well as an ITU-T recommendation. Its rich feature list includes progressive transmission by quality, resolution, component, or spatial locality, lossy and lossless compression, region of interest coding by progression, and limited memory implementations, to name a few. The JPEG2000 encoder consists of three main stages: discrete wavelet transform, scalar quantization, and block coding. After the DWT stage, embedded scalar quantization is performed with the quantization step size possibly varying for each subband. The block coder is based on the principles of Embedded Block Coding with Optimized Truncation (EBCOT) (Taubman, 2000) and includes an arithmetic coder coupled with a rate-distortion optimization algorithm to achieve the optimal bit rates.

3.2 Predictor Based Schemes: CALIC and JPEG-LS are the state-of-the-art lossless compression schemes that belong to this class of compression schemes. Both of these are characterized by prediction of the current pixel value using some of its previous neighbors, and then entropy coding of the error between the predicted value and actual pixel value.

3.2.1 CALIC: The CALIC scheme is considered as the most efficient and complex encoder for compression of 2D continuous-tone images. Among the nine proposals in the initial ISO/JPEG evaluation in July 1995, CALIC was ranked first. It works on the principle of a context-adaptive non-linear predictor which adjusts to the local gradients around the current pixel. A schematic description of the coding algorithm from the original paper (Wu 1997), is shown in Fig. 6. The algorithm operates in the binary or continuous modes. The binary mode codes the regions of the image in which the intensity value is no more than two. In the continuous mode, the system has four major components: gradient-adjusted prediction, context selection and quantization, context modeling of prediction errors, and entropy coding of prediction errors.

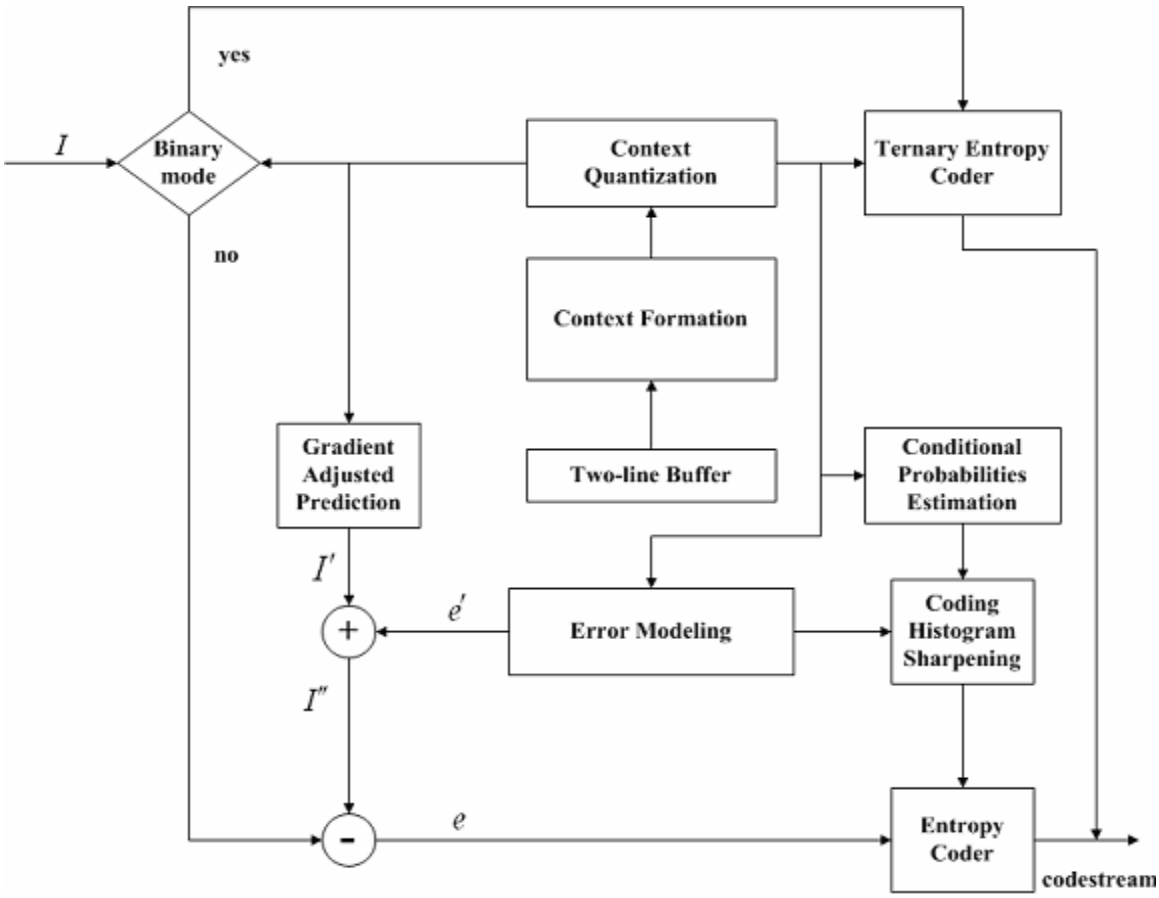

Fig. 6. Schematic description of CALIC's encoder.

3.2.2 JPEG-LS: The ISO/IEC working group released a new standard for the lossless/ near lossless compression of continuous-tone images in 1999, popularly known as JPEG-LS[8]. It features low complexities based on predictive coding technique. Near lossless compression is controlled through an integer valued threshold representing the maximum permissible absolute difference between each original pixel value and its decompressed value. As shown in Fig. 7, the JPEG-LS encoder is composed of four main stages: prediction, context modeling, error encoding, and run mode.

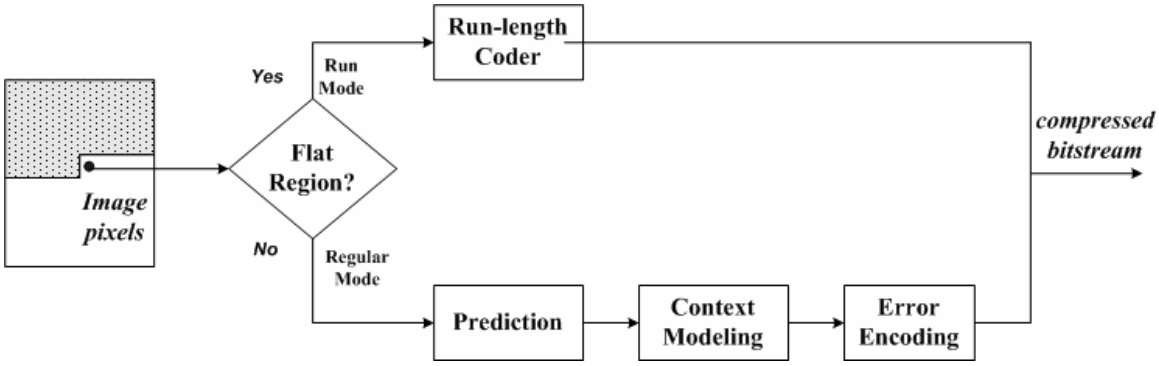

Fig. 7. Schematic description of JPEG-LS's encoder.

4. RESULTS

Ten 3D granules are studied in this paper for lossless hyperspectral sounding data compression. Different 3D integer wavelet transforms are used together with zerotree coding such as EZW and SPIHT for compression of these granules. The compression ratios obtained for both these schemes is depicted in Fig. 8. For the wavelet transform, we use the notation $L/\tilde{L}$ to represent the length of the low pass and high pass filters respectively. Additionally, we also represent the wavelet transform by a pair of vanishing moments $(n, \tilde{n})$, where n and $\tilde{n}$ represent the number of vanishing moments of the analysis and the synthesis high pass filters respectively.

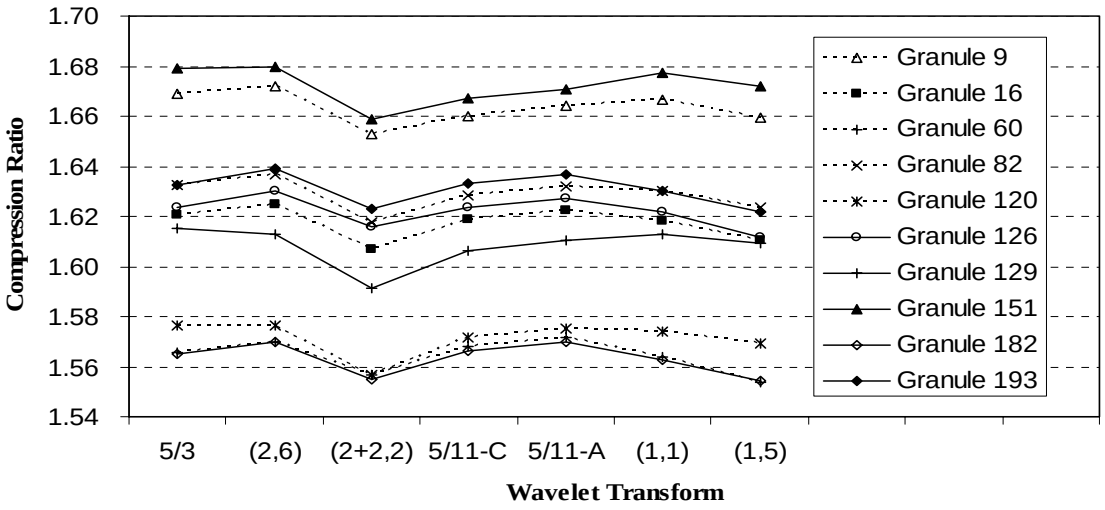

(a)

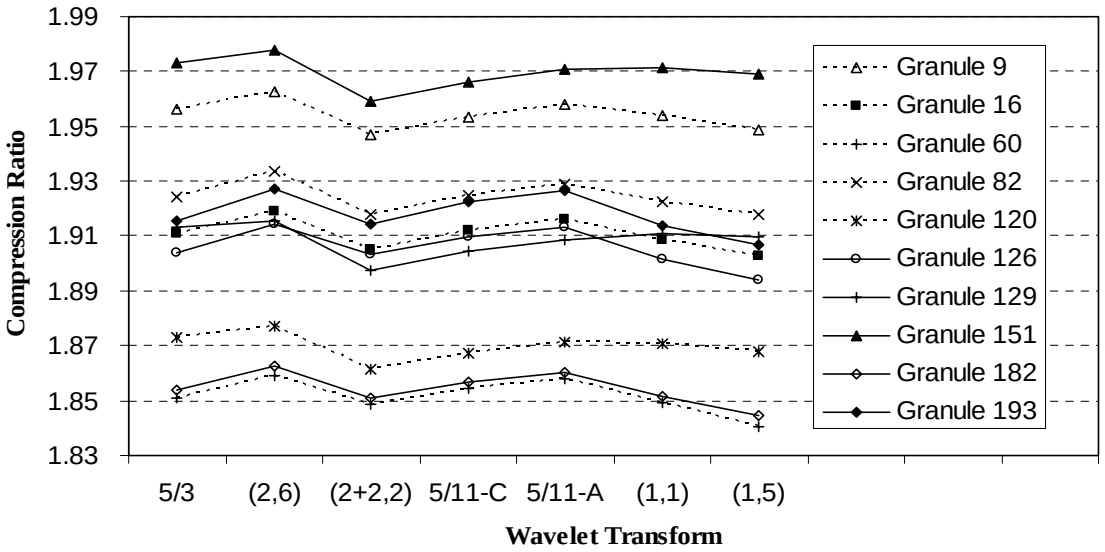

(b)

Fig. 8. (a) Compression ratios for 3D EZW with different wavelet transforms for the 10 tested granules. (b) Same as (a) except for 3D SPIHT.

Since JPEG2000 (Part I), CALIC and JPEG-LS only support compression of 2D data, each granule with the size of 2108 channels by 135 scan lines by 90 footprints is converted into 2D with the size of 2108 channels by 12150 samples via a horizontal zigzag continuous scan. This continuous scan will make smooth the transition of the data samples from one line to another. For the 3D EZW and 3D SPIHT compression schemes, the granules are used in their original 3D form of 2108 channels by 135 scan lines by 90 footprints for compression. Table 2 shows the bit rates achieved for all the ten granules.

granule no.	CALIC	JPEG-LS	JPEG2000	3D EZW	3D SPIHT
9	8.8839	8.0385	8.1972	9.5711	8.1516
16	9.0310	8.2394	8.4349	9.8480	8.3368
60	9.3528	8.4442	8.6900	10.1820	8.6063
82	8.9630	8.2071	8.3694	9.7740	8.2760
120	9.0065	8.4404	8.5904	10.1491	8.5233
126	9.2698	8.2538	8.4515	9.8166	8.3590
129	8.7985	8.2741	8.3934	9.9053	8.3520
151	8.6992	7.9398	8.0781	9.5238	8.0898
182	9.3401	8.4794	8.6994	10.1917	8.5906
193	9.1553	8.2304	8.4222	9.7626	8.3026

Table 2. Bit rates for the various compression for the 10 tested granules.

Alternatively, the compression results can be represented in terms of compression ratios as illustrated in Fig. 9.

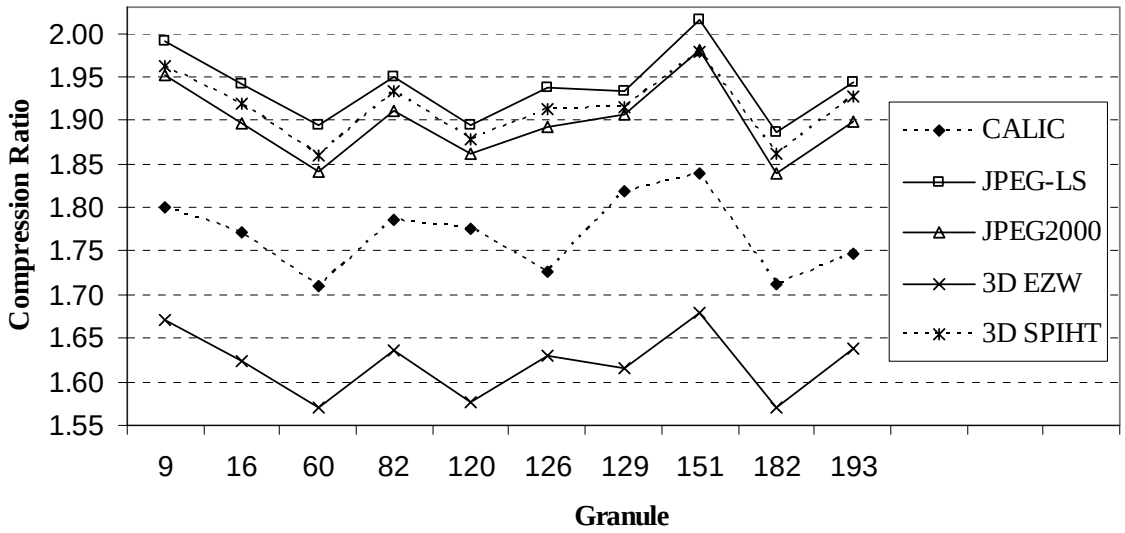

Fig. 9. Compression ratios for the various compression for the 10 tested granules.

As seen in Fig. 9, JPEG-LS produces the highest compression ratios when compared to all the other schemes. 3D SPIHT outperforms JPEG2000 by a small margin, whereas the

3D EZW scheme has the lowest compression ratios. JPEG-LS also has the lowest complexity in terms of algorithm design among all of the compression schemes.

5. SUMMARY

The hyperspectral sounding data is a new class of 3D data for compression studies. The compression of this data is better to be lossless or near lossless to avoid significant degradation of the geophysical retrieval. In this paper lossless compression of the 3D hyperspectral sounding data is performed using wavelet transform based and predictor based compression schemes. A comparison of these schemes including 3D EZW, 3D SPIHT, JPEG2000 (wavelet transform based) and CALIC, JPEG-LS (predictor based) in terms of compression ratios is given. The results show that JPEG-LS outperforms all the other schemes in terms of compression ratios for the ten granules of the AIRS hyperspectral data representing different geographical locations of the earth.

ACKNOWLEDGEMENT

The authors would like to thank Dr. Elisabeth Weisz for providing the original AIRS data. This research is supported by National Oceanic and Atmospheric Administration's National Environmental Satellite, Data, and Information Service under grant NA07EC0676.

References

Abousleman G.P., 1999: Adaptive coding of hyperspectral imagery in Proceedings of the 1999 IEEE International Conference on Acoustics, Speech, and Signal Processing, 2243 -2246.

Aumann H.H. and Strow L., 2001: AIRS, the first hyperspectral infrared sounder for operational weather forecasting in Proceedings of IEEE Aerospace Conference, 1683-1692.

Bloom H.J., 2001: The Cross-track Infrared Sounder (CrIS): a sensor for operational meteorological remote sensing in Proceedings of the 2001 International Geoscience and Remote Sensing Symposium, 1341-1343.

Daubechies I. and Sweldens W., 1998: Factoring wavelet and subband transforms into lifting steps in *J. Fourier Anal. Applica.*, **4**, 245-267.

Huang B., Huang H.L., Chen H., Ahuja A., Baggett K., Smith T.J., Heymann R.W., 2003: Data Compression Studies for NOAA Hyperspectral Environmental Suite (HES) using 3D Integer Wavelet Transforms with 3D Set Partitioning in Hierarchical Trees presented at the SPIE International Symposium on Remote Sensing Europe, Barcelona, Spain, 8-12 Sept. 2003.

ISO/IEC 15444-1, 2000: Information technology - JPEG2000 image coding system-part 1: Core coding system.

ISO/IEC 14495-1 and ITU Recommendation T.87, 1999: Information Technology – lossless and near-lossless compression of continuous-tone still images.

Phulpin T., Cayla F., Chalon G., Diebel D., and Schlüssel D., 2002: IASI onboard Metop: Project status and scientific preparation presented at the Twelfth International TOVS Study Conference, Lorne, Victoria, Australia, 26 February-4 March 2002.

Said A. and Pearlman W. A., 1996: A new, fast, and efficient image codec based on set partitioning in hierarchical trees in *IEEE Trans. Circuits and Systems for Video Technology*, **6**, 243-250.

Shapiro J. M., 1993: Embedded image coding using zerotrees of wavelet coefficients in *IEEE Trans. Signal Processing*, **41**, 3445-3462.

Smith W.L., Harrison F.W., Hinton D.E., Revercomb H.E., Bingham G.E., Petersen R., and Dodge J.C., 2002: GIFTS - the precursor geostationary satellite component of the future earth observing system in Proceedings of the 2002 International Geoscience and Remote Sensing Symposium, 357-361.

Taubman D., 2000: High performance scalable image compression with EBCOT in *IEEE Trans. Image Proc.*, **9**, 1158-1170.

Wu X., 1997: Lossless compression of continuous-tone images via context selection, quantization, and modeling in *IEEE Trans. on Image Proc.*,**6**, 656–664.